



Research article

Identification of cellular senescence-associated genes as new biomarkers for predicting the prognosis and immunotherapy response of non-small cell lung cancer and construction of a prognostic model

Dandan Xu ^{a,b}, Xiao Chen ^b, Mingyuan Wu ^c, Jinfeng Bi ^a, Hua Xue ^b, Hong Chen ^{a,*}

^a Department of Respiratory and Critical Care Medicine, The Second Affiliated Hospital of Harbin Medical University, Harbin, China

^b Department of Geriatric Respiratory Medicine, Heilongjiang Provincial Hospital, Harbin, China

^c Center for Disease Control and Prevention, Songbei District, Harbin, China

ARTICLE INFO

Keywords:

Non-small cell lung cancer
Cellular senescence
Risk score
Prognostic model

ABSTRACT

Background: Globally, lung carcinoma remains the leading cause of death, with its associated morbidity and mortality rates remaining elevated. Despite the slow advancement of treatment, the outlook remains bleak. Cellular senescence represents a halt in the cell cycle, encompassing a range of physiological and pathological activities, along with diverse phenotypic alterations, including variations in secretory phenotype, macromolecular harm, and metabolic disturbances. Research has revealed its vital function in the formation and growth of tumors. This study aimed to examine cellular senescence-related mRNAs linked to the outlook of non-small cell lung cancer (NSCLC) and to formulate a predictive risk framework for NSCLC.

Methods: We acquired the NSCLC expression data from The Cancer Genome Atlas (TCGA) to examine mRNAs linked to cellular senescence. Both single-variable and multiple-variable cox proportion risk assessments were utilized to determine the traits of cellular senescence-related mRNAs linked to NSCLC prognosis. Subsequently, the prognostic model for cellular senescence-related mRNAs was integrated with clinical-pathological characteristics to create a prognostic nomogram. Furthermore, the study delved into the risk-oriented predictive model, examining immune infiltration and responses to immunotherapy among both high and low-risk categories. **Results:** Utilizing both univariate and multivariate Cox proportion risk assessments, a risk model comprising 12 mRNAs associated with cellular aging was ultimately developed: *IGFBP1*, *TLR3*, *WT1*, *ID1*, *PTTG1*, *ERRFI1*, *HEPACAM*, *MAP2K3*, *RAD21*, *NANOG*, *PRKCD*, *SOX5*. Univariate analysis and multivariate analysis illustrated that the risk score served as a standalone indicator for prognosis, and the hazard ratio (HR) of the risk score were 1.182 (1.139–1.226) ($p < 0.001$) and 1.162 (1.119 – 1.206) ($p < 0.001$), respectively. Individual prognoses were forecasted using nomogram, c-index, and principal component analysis (PCA). Furthermore, the risk-oriented model revealed notable statistical variances in immune infiltration and response to immunotherapy among the high and low risk categories.

Conclusions: This study shows that mRNAs related to cell senescence associated with prognosis are reliable predictors of NSCLC immunotherapy reaction and prognosis.

* Corresponding author.

E-mail addresses: xudandan199122@hotmail.com (D. Xu), chenhong744563@aliyun.com (H. Chen).

1. Introduction

Lung carcinoma is a malignant tumor originating from lung gland or bronchial mucosa. Considering the worldwide cancer data from 2020, it's estimated that there are 2.3 million new instances and 1.8 million fatalities due to lung cancer [1]. Lung cancer is the leading cause of morbidity and mortality in China, and this situation may deteriorate with socio-economic transformation and population aging [2–4]. The predominant pathological form of lung cancer is non-small cell lung cancer, constituting 85% of all lung cancer cases, predominantly adenocarcinoma and squamous cell carcinoma. The predicted 5-year relative survival rates of newly diagnosed squamous cell carcinoma and adenocarcinoma histological cases are only 32.2% and 24.2%, respectively [5]. NSCLC is closely related to different risk factors, including gene mutation, tobacco consumption, chronic or dysfunctional inflammation, immune dysfunction and so on, which may increase the incidence of lung cancer [6]. NSCLC has no specific clinical symptoms in the early stage, mostly diagnosed in the middle and late stages, and is prone to invasion or metastasis. Although there are single or combined therapies such as chemotherapy, radiotherapy, and targeted therapy, with the emergence of immunotherapy in recent years, this treatment model has been broken and has become a promising choice. However, the efficacy of immunotherapy is affected by tumor mutation load (PD-L1 expression) [7], infection [8], drugs [9–13], gender [14], diet [15] and other factors. While the solitary or combined use of targeted therapy or immunotherapy has advanced significantly in clinical settings, the five-year survival rate for advanced NSCLC remains alarmingly low, not exceeding 15% [16]. Therefore, there is an immediate necessity to investigate novel biomarkers for forecasting the advancement, future outlook, and reaction to NSCLC treatment.

Cellular senescence refers to a halt in the cell cycle, encompassing numerous physiological and pathological mechanisms. Hayflick and Moorhead initially noted in 1961 the restricted division propensity of mammalian cells, termed the 'Hayflick limit' [17]. A range of stress factors can lead to cellular aging, such as contact with genotoxic agents, DNA impairment, lack of nutrition, oxygen deprivation, mitochondrial malfunction, and activation of oncogenes [18–23]. The process of cellular aging can occur during any stage of life. Beyond halting the cell cycle, numerous phenotypic alterations exist, including changes in secretory phenotypes, macromolecular harm, and metabolic irregularities [24]. The aging of cells could serve as a mechanism for the body's self-defense. Intricate mechanisms like the reduction of telomere length or clashes in growth signals compel atypical cells to transition into the irreversible G0 phase, thereby halting their growth and preventing endless multiplication of cancer cells [25–27]. The process of cellular aging exhibits various alterations, including increased levels of cell cycle inhibitors, modifications in cellular architecture, and shifts in protein production. Aging cells proliferate to nearby healthy and cancerous cells through the emission of senescence-related secretory phenotypes (SASP) or by releasing various pro-inflammatory agents, chemokines, growth factors, proteases, and additional paracrine processes [28]. This factor influences tumor blood vessel formation, cell growth, resistance to chemotherapy, the shift from epithelial to mesenchymal cells, stem cell regeneration/differentiation, and tissue healing [18,29]. As one ages, there's a gradual decline in lung capacity, marked by structural alterations that hinder gas exchange and immune responses, increasing vulnerability to infections. Aging is indicated by cellular aging, marked by a diminished capacity to react to environmental pressures. For many years, it has been believed that malignant tumors are caused by the accumulation of multiple mutations in somatic cells. The increase of resident senescent cells in the senescent lung leads to a decrease in immune surveillance function, which may enhance the inherent mitotic changes of other cells and eventually lead to lung cancer [30]. However, how cellular senescence manipulates innate and acquired immune responses to influence the development of end-organ lung cancer and lung cancer remains unclear. For decades, some researchers have tried to find new targeted therapy strategies and tumor prognosis through the study of cellular senescence.

This research developed a gene profile, risk score, and prognosis model for cellular senescence-related mRNAs to methodically assess the relationship between these mRNAs and the prognosis of NSCLC patients, including their clinicopathological traits. Subsequently, we created a nomogram that merges features of cellular aging-related mRNAs with clinical elements to predict the duration of survival, immune status, and response to immunotherapy in these patients. The findings of our study offer crucial understanding of how cells age in NSCLC, potentially enhancing the efficacy of personalized treatments and prognostic analysis.

2. Materials and methods

2.1. Data set extraction

Lung cancer RNA-sequencing (RNA-seq) data was sourced from The Cancer Genome Atlas (TCGA) database (<https://portal.gdc.cancer.gov/>). Based on the set criteria for inclusion, the study encompassed a total of 941 patients diagnosed with NSCLC. Criteria for inclusion included: (1) NSCLC (encompassing adenocarcinoma and squamous cell carcinoma); (2) comprehensive transcriptome data and clinical details, excluding samples with a follow-up period not exceeding 30 days during clinical evaluations. The genes exhibiting the greatest expression were chosen as gene symbols and annotated using the human.gtf. Annotation package.

Genes linked to cellular aging were sourced from the CellAge database (<https://genomics.Sene-science.info/cells/>). The 'limma' software package in R was employed to isolate the expression patterns of intersecting genes for the purpose of differential analysis. Criteria for the filter included: $p < 0.05$ and $|\log_2FC| > 1$. Genes responsible for varying cellular aging in NSCLC were identified, and the differential analysis outcomes were depicted as a heatmap using R software's 'pheatmap' package. Given that this study encompasses all information from the TCGA database and adheres rigidly to the guidelines provided by TCGA (<http://cancergenome.nih.gov/abouttcga/policies/publicationguidelines>), it proceeds without the consent of the ethics committee.

2.2. Functional enrichment analysis

Gene function analysis employed Gene Ontology (GO) and Kyoto Encyclopedia of Genes and Genomes (KEGG) enrichment analysis to further verify the possible roles of the target genes. With the purpose of better comprehend the carcinogenic effects of target genes, we used the Cluster Profiler package in 'R' to analyze the role of potential mRNAs in GO and the enrichment of the KEGG pathway.

2.3. Construct a prognostic model

Initially, the predictive value of mRNAs linked to cellular aging was assessed using univariate Cox regression analysis. Subsequently, through univariate analysis, notable mRNAs linked to prognostic cellular aging were pinpointed, meeting a significance level of $p < 0.05$. Subsequently, key genes underwent additional screening through the least absolute shrinkage selection operator (LASSO) regression analysis, a technique enhancing the predictive precision and clarity of statistical models via variable selection and regularization [31]. The confidence interval for each lambda was calculated using a 10-fold cross-validation method and then we determined the best lambda with the lowest average error [32,33]. Following this, stepwise multivariate Cox regression analysis was employed to pinpoint crucial genes linked to prognosis and develop an optimal prognostic risk model. Our assumption was that genes chosen by p were fed into a predictive model for prognosis, denoted as (x_1, \dots, x_p) . The risk score constituted a weighted aggregate of genes, with its weight indicating the level of association, termed as the risk score = $\beta_1 \times x_1 + \dots + \beta_p \times x_p$ (β is the coefficient value, and x represents the expression level of chosen mRNAs). Patients were categorized into two segments, high-risk and low-risk, based on their median risk scores. Survival variances between the two groups were analyzed using the log-rank test. An independent prognostic model was created using Cox regression, and a nomogram was employed to forecast patient survival rates, verifying if the risk score served as an independent prognostic marker.

2.4. Prognostic valuation of mRNAs model associated with cellular senescence

Out of the 941 samples, they were randomly split into two segments: a training set comprising 472 cases and a validation set with 469 cases. Utilizing the prognostic risk model, each patient's risk score was recorded, categorizing them into high-risk and low-risk groups. The Kaplan-Meier method for survival analysis was employed to evaluate the variance in survival rates between groups with high and low risk. The predictive capacity of gene markers and diverse clinicopathological characteristics was assessed using time-based ROC curve analysis. To forecast overall survival (OS) in NSCLC patients, a nomogram was developed, incorporating clinicopathological characteristics such as age, gender, stage, TMN stage and risk assessments based on prognostic elements. The C-index and the calibration curve served as tools to assess the nomogram's forecasting capacity.

2.5. Principal component analysis

Principal component analysis (PCA) was employed to evaluate how patients varied in risk scores. Every gene, along with mRNAs linked to cell aging and model mRNAs, were rendered visible, simplifying the gene count into three distinct dimensions: PC1, PC2, and PC3. Samples categorized as high-risk and low-risk were denoted in yellow and blue, in that order. The R software package 'limma' along with scatterplot3D were employed for PCA generation.

2.6. GSEA functional analysis

The function of gene expression data was investigated using gene set enrichment analysis (GSEA, <http://www.broadinstitute.org/gsea/index.jsp>). Our investigation delved into the enhanced functionality of mRNAs linked to cellular aging, which hold predictive significance, and identified the leading 10 GO and KEGG pathways.

2.7. Immune infiltration analysis

CIBERSORT was employed for analyze immune cell infiltration, refined using the Perl programming language, to derive the immune cell infiltration matrix. Adjustments were made to the P-value below 0.05 based on the cutoff standard, utilizing the 'barplot', 'corrplot', and 'gplot2' tools in R language version 4.1.0 for sample visualization. The 'corrplot' software was utilized to determine the correlation between the gene expression matrix and immune cells.

2.8. Analysis of immune function and immune cells in high and low risk groups

The ssGSEA technique, a single sample Gene Set Enrichment Analysis, was employed to measure various tumor-infiltrating immune cell subsets and assess their immune roles across both groups. The source of the immune.gmt file is <http://www.gsea-msigdb.org/gsea/index.jsp>, which houses genes related to immune cells and functions. Data on gene expression were transformed into information on immune function and cell scores using gene acquisition files.

2.9. Differences of immune checkpoint expression in high-risk and low-risk populations

Genes linked to immune checkpoints were sourced from the cited references. The analysis of immune checkpoints utilized the R software's 'limma' package, 'shape2' package, 'ggplot2' package, 'gpubr' package, and 'beeswarm' package. Genes exhibiting notable variances were isolated, and upon reaching $p < 0.05$, an analysis was conducted on the disparities in immune checkpoint levels between high-risk and low-risk samples.

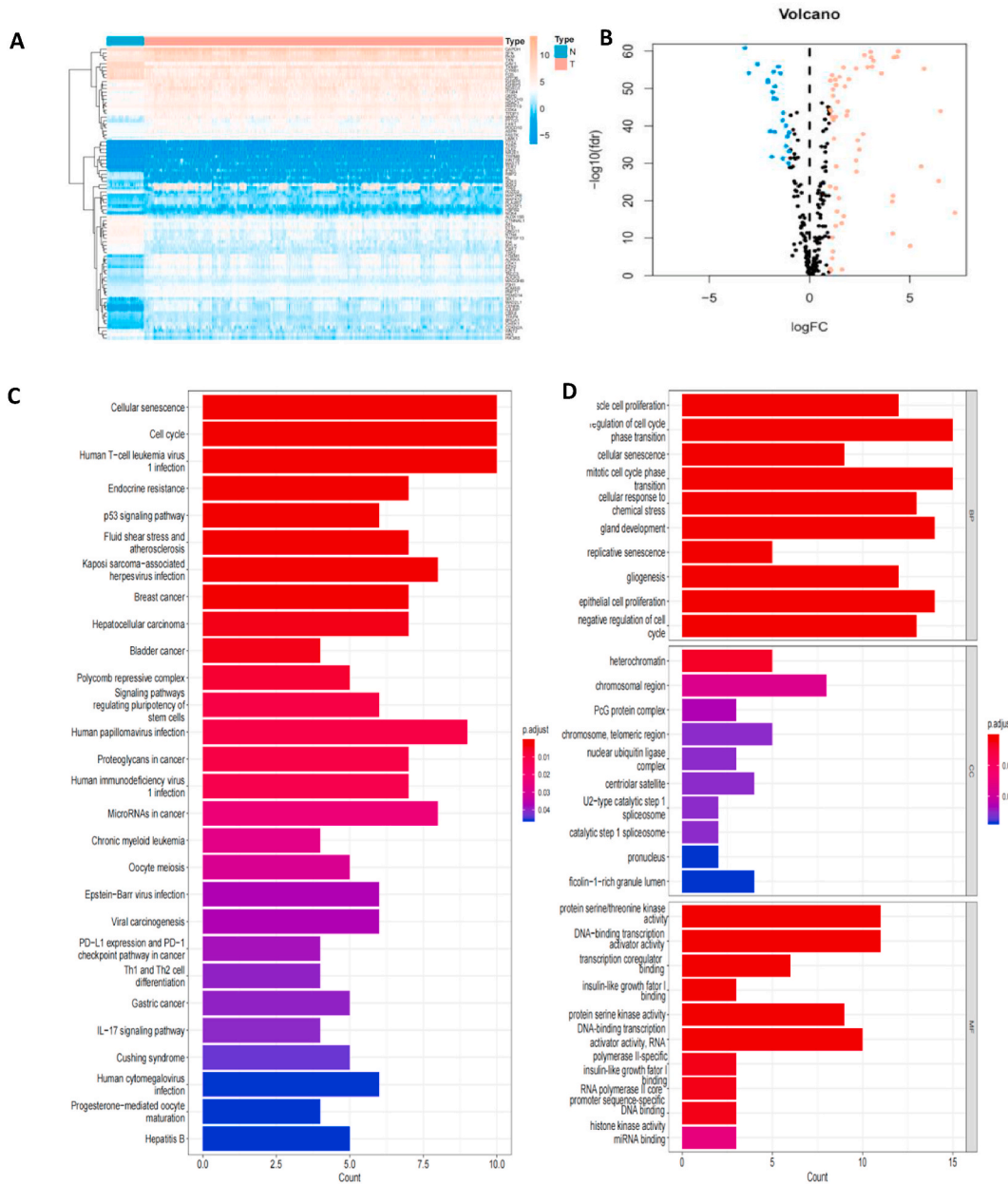


Fig. 1. Analysis of DEGs and functional enrichment linked to cellular aging. (A) A heatmap representation of 82 genes linked to cell senescence in NSCLC. (B) A volcanic chart depicting 82 genes linked to cell senescence in NSCLC. Genes that are upregulated are indicated by red dots, while those downregulated are shown by blue dots. (C) Examination of DEGs linked to cellular aging through KEGG. (D) Gene Ontology examination of DEGs linked to cellular aging. (For interpretation of the references to colour in this figure legend, the reader is referred to the Web version of this article.)

2.10. Statistical analysis

The research employed R (4.1.0) for analyzing data. A p-value less than 0.05 was deemed to indicate statistically significant variances.

3. Results

3.1. Detecting genes with differential expression linked to cellular senescence in NSCLC and conducting an analysis of functional enrichment

The CellAge database yielded 279 genes associated with cellular aging. Expression levels of 274 genes were extracted from the NSCLC dataset (Table S1), followed by an analysis of the DEGs against RNA-seq data from both NSCLC samples and normal tissues ($|\log_2FC| > 1.0$ and $p < 0.05$). Screening was conducted on 82 differentially expressed genes (Fig. 1A, Table S2), encompassing 58 genes with increased expression and 24 with decreased expression (Fig. 1B).

KEGG and GO analyses were conducted on differentially expressed genes associated with cell aging. In KEGG analysis, a total of 15 pathways were significantly enriched. Analysis of the KEGG pathway revealed a predominant presence of DEGs associated with

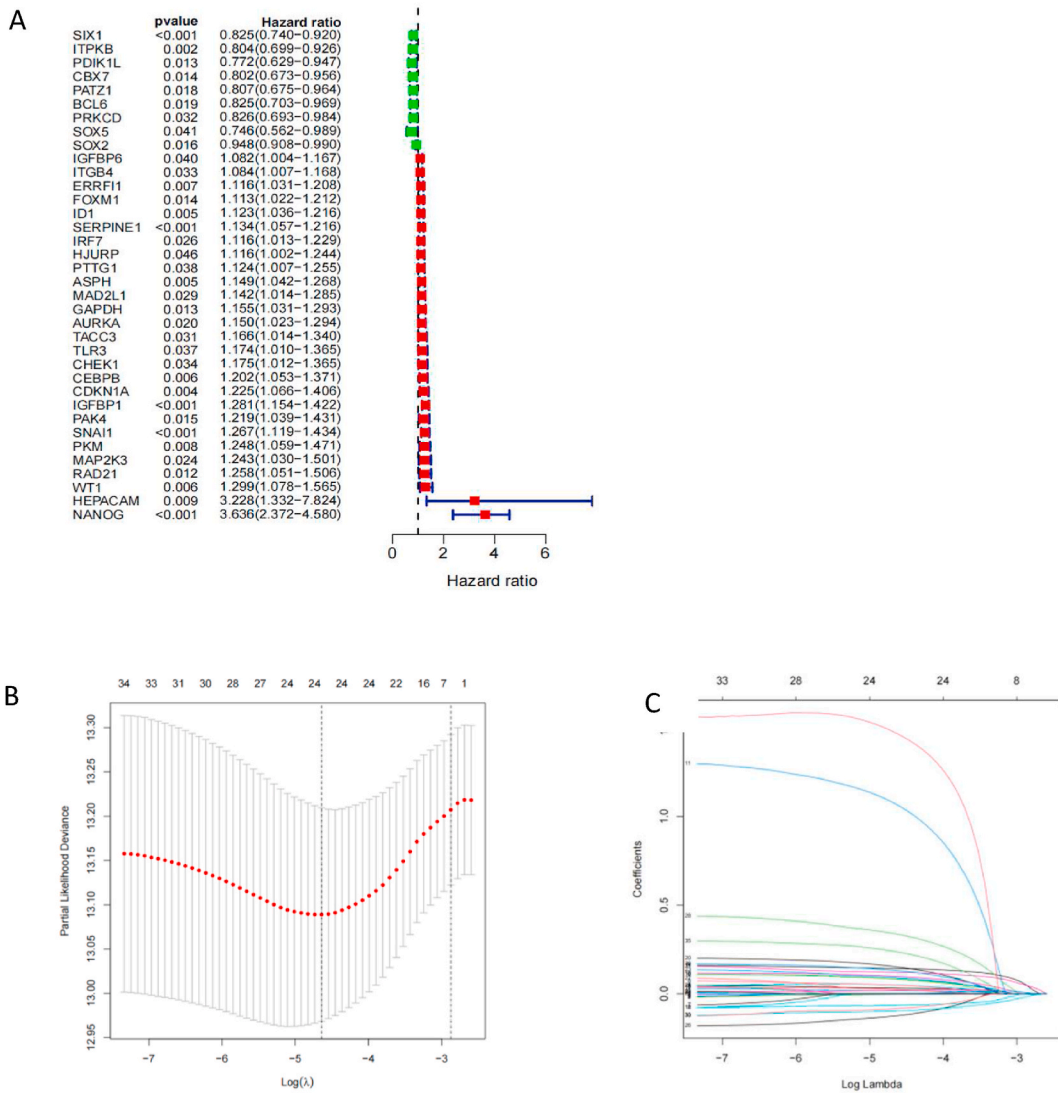


Fig. 2. Depicts the development of a model predicting cell senescence. (A) Detecting mRNAs linked to cell aging that hold substantial predictive importance in NSCLC. A forest graph displays the hazard ratios (95% confidence interval) and probability values for chosen mRNAs, ascertained through univariate Cox proportional hazards analysis (all $p < 0.05$). The red marker indicates the hazard ratio (HR) for mRNAs exceeding 1, while the green marker denotes HR below 1. (B-C) The LASSO Cox regression model was employed to develop the risk score system. (For interpretation of the references to colour in this figure legend, the reader is referred to the Web version of this article.)

cellular senescence, cell cycle, human T-cell leukemia virus 1 infection, p53 signaling pathway, etc. The findings imply that these communication routes could be crucial in the emergence and advancement of NSCLC, and these DEGs may be potential therapeutic targets or biomarkers. Further study of the function and interaction of these signaling pathways and genes will aid in comprehending the molecular workings of NSCLC and offer fresh perspectives for diagnosing and treating patients. (Fig. 1C–Table S3).

GO analysis in the realm of biological processes revealed a predominant enrichment of DEGs in areas such as muscle cell growth, control of cell cycle phase changes, and cellular aging. Within the category of cellular components, DEGs predominantly showed enrichment in areas like heterochromatin, chromosomal regions, and the PcG protein complex, among others. Within the realm of molecular functions, DEGs predominantly showed an increase in activities like protein serine/threonine kinase, DNA-binding transcription activator, transcription coregulator binding, and more. (Fig. 1D–Table S4). Consequently, these routes are crucial in the progression of lung cancer. Delving deeper into the crucial genes within these pathways and their interplay methods will enhance our comprehension of lung cancer's development.

3.2. Development of a prognostic model related to cellular senescence

First, through univariate Cox regression analysis, we pinpointed 36 mRNAs linked to cellular senescence and cancer risk ($p < 0.05$). Among them, 9 cellular senescence-related mRNAs served as protective elements ($HR < 1$), while 27 were identified as high-risk factors ($HR > 1$) (Fig. 2A).

Then, through LASSO regression analysis, 24 mRNAs were further screened and listed in the following analysis. Multivariate Cox regression analysis obtained 1 mRNA and established a prognostic model. A total of ten mRNAs were deemed as unfavorable prognostic indicators, while two mRNAs were recognized as positive prognostic factors. These mRNAs were used to establish cellular senescence-associated mRNA models. The method to compute the risk score is outlined below: $(PRKCD \times -1.05654918) + (SOX5 \times -0.381873764) + (IGFBP1 \times 0.337423173) + (TLR3 \times 0.442640427) + (WT1 \times 0.548856678) + (ID1 \times 0.674047922) + (PTTG1 \times 0.695511779) + (ERRFI1 \times 0.740068853) + (HEPACAM \times 1.369239984) + (MAP2K3 \times 1.40456484) + (RAD21 \times 1.466722664) + (NANOG \times 1.887767634)$ (Fig. 2B and 2C; Table 1).

3.3. Effect of the established model on prognosis

To showcase the foreseeability of the cellular senescence-related mRNAs model, patient risk scores were recorded in both the training and validation datasets (Figs. 3A and 4A). Within the training and validation datasets, NSCLC patients in the high-risk category exhibited greater mortality rates compared to those in the low-risk category (training set 110/236 vs 57/236; validation set 89/211 vs 82/258) (Figs. 3B and 4B). Across both groups, the overall survival rate for patients at high risk was less compared to those at low risk (Figs. 3C and 4C). Furthermore, the ROC curve's area under the curve (AUC) for 1-, 3-, and 5-year survival rates stood at 0.683, 0.709, and 0.672 in the training group, and 0.619, 0.676, and 0.637 in the validation group, respectively, indicating that this feature has good predictive performance (Figs. 3D and 4D).

3.4. Correlation between differential expression of cellular senescence-related genes and clinicopathological variables

We performed a univariate analysis of 12 cellular senescence-related mRNAs and divided patients into high and low expression group based on the expression of individual genes. We also observed a significant difference in OS ($p < 0.05$). According to the heatmap, there was a significant difference in age (> 65), sex, T stage and survival status ($p < 0.05$) (Fig. 5A–5C). However, we did not find any significant differences in age (≤ 65), N stage, and M stage (Fig. 5B).

Table 1

Multivariate Cox regression construct a prognostic model.

id	coef	HR	HR.95L	HR.95H	pvalue
ERRFI1	0.74	2.10	1.24	3.54	0.0057
HEPACAM	1.37	3.93	0.98	15.70	0.0526
ID1	0.67	1.96	1.18	3.27	0.0098
IGFBP1	0.34	1.40	1.04	1.89	0.0271
MAP2K3	1.40	4.07	1.50	11.10	0.0060
NANOG	1.89	6.60	1.70	25.63	0.0064
PRKCD	-1.06	0.35	0.12	0.98	0.0452
PTTG1	0.70	2.00	1.05	3.81	0.0340
RAD21	1.47	4.34	1.09	17.19	0.0369
SOX5	-0.38	0.68	0.42	1.12	0.1297
TLR3	0.44	1.56	1.06	2.30	0.0257
WT1	0.55	1.73	1.19	2.52	0.0042

Coef: refers to the coefficient of mRNAs that is associated with survival rates. **HR:** stands for hazard ratio. **HR. 95L:** low 95% confidence interval for hazard ratio. **HR. 95H:** high 95% confidence interval for hazard ratio.

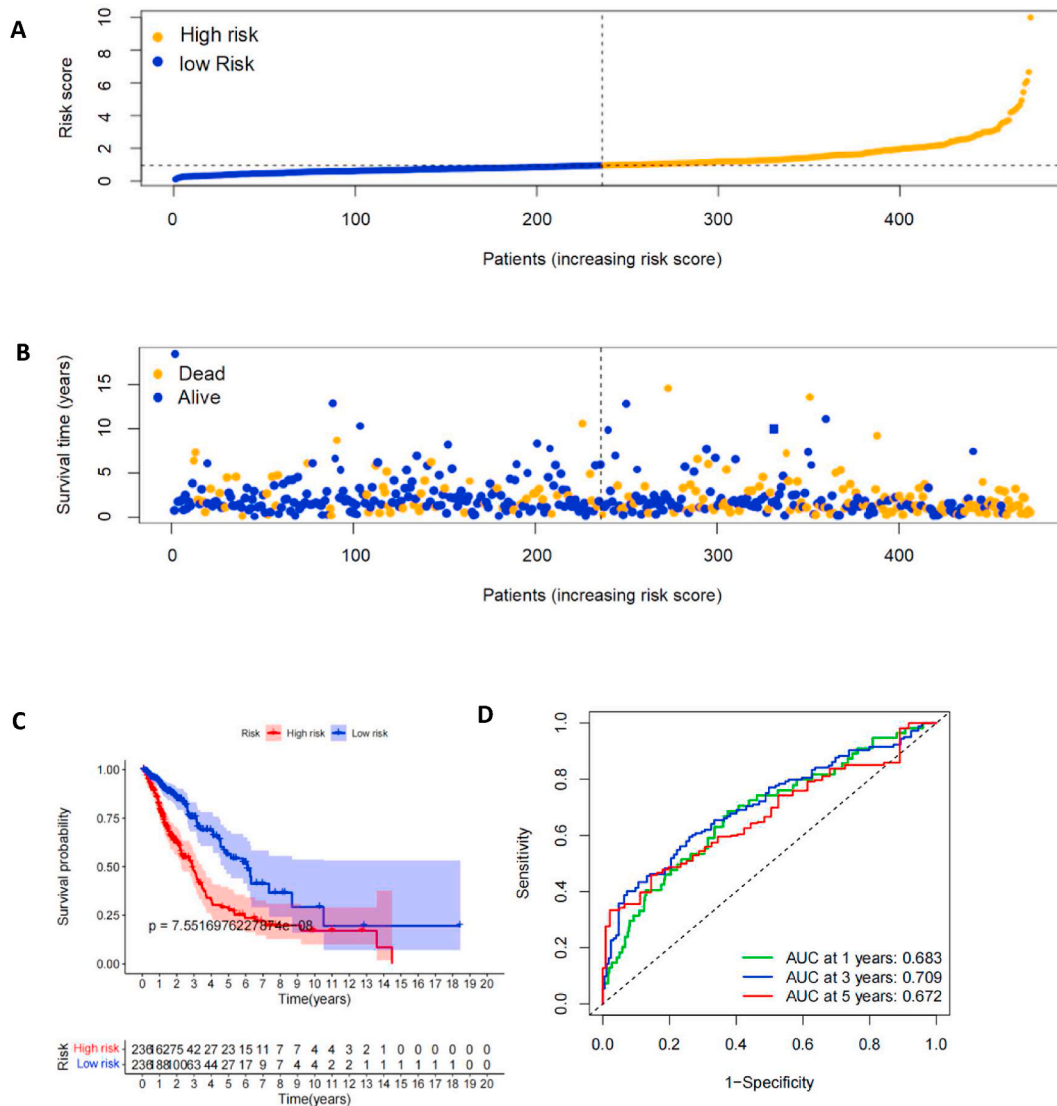


Fig. 3. Evaluation of signature within the training dataset. (A) Allocation of risk ratings between high and low risk categories. High-risk and low-risk were indicated by orange and blue points, in that order. **(B)** Allocation of survival rates among NSCLC patients categorized into high/low risk groups. A blue dot signified life and an orange dot denoted death. **(C)** Curve depicting survival. The survival rates of the high and low risk groups were depicted by the red and blue lines, in that order. **(D)** ROC Curve. (For interpretation of the references to colour in this figure legend, the reader is referred to the Web version of this article.)

3.5. Confirming the predictive model and developing a nomogram focused on mRNAs associated with cellular senescence

Results from the univariate Cox regression analysis indicated that outcomes were independently predicted by both the risk score and stage, with a hazard ratio (HR) of 1.182 (95% CI 1.139–1.226) for these scores (Fig. 6A). Within the range of multivariate clinical features, the risk score stood out as a standalone predictor in the multivariate analysis (1.162 (95% CI 1.119–1.206), $P < 0.001$) (Fig. 6B). Subsequently, the nomogram incorporated risk score, age, and TNM stage. With an AUC score of 0.657, surpassing other clinical pathological characteristics (Fig. 6C), it's deduced that 12 mRNAs linked to cellular senescence are reliably reliable for predicting NSCLC risk. As shown in the nomogram, the prognosis of NSCLC patients is most significantly influenced by the risk score (Fig. 6D). As the stage progressed, the risk score escalated, indicating the potential role of mRNAs signals linked to cellular aging in the advancement of NSCLC. Furthermore, the risk score was employed to develop a nomogram, utilizing the expression of 12 risk-associated mRNAs as variables, to forecast each patient's overall survival rate. The calibration graph revealed the nomogram's strong predictive capacity, with the risk score nomogram's c-index surpassing that of other clinical variables (Fig. 6E–G). Collectively, these findings suggest that the risk score accurately forecasts the prognosis of NSCLC. Such information could assist medical professionals in making informed clinical choices for individuals with NSCLC, offering crucial perspectives for tailoring treatment to each

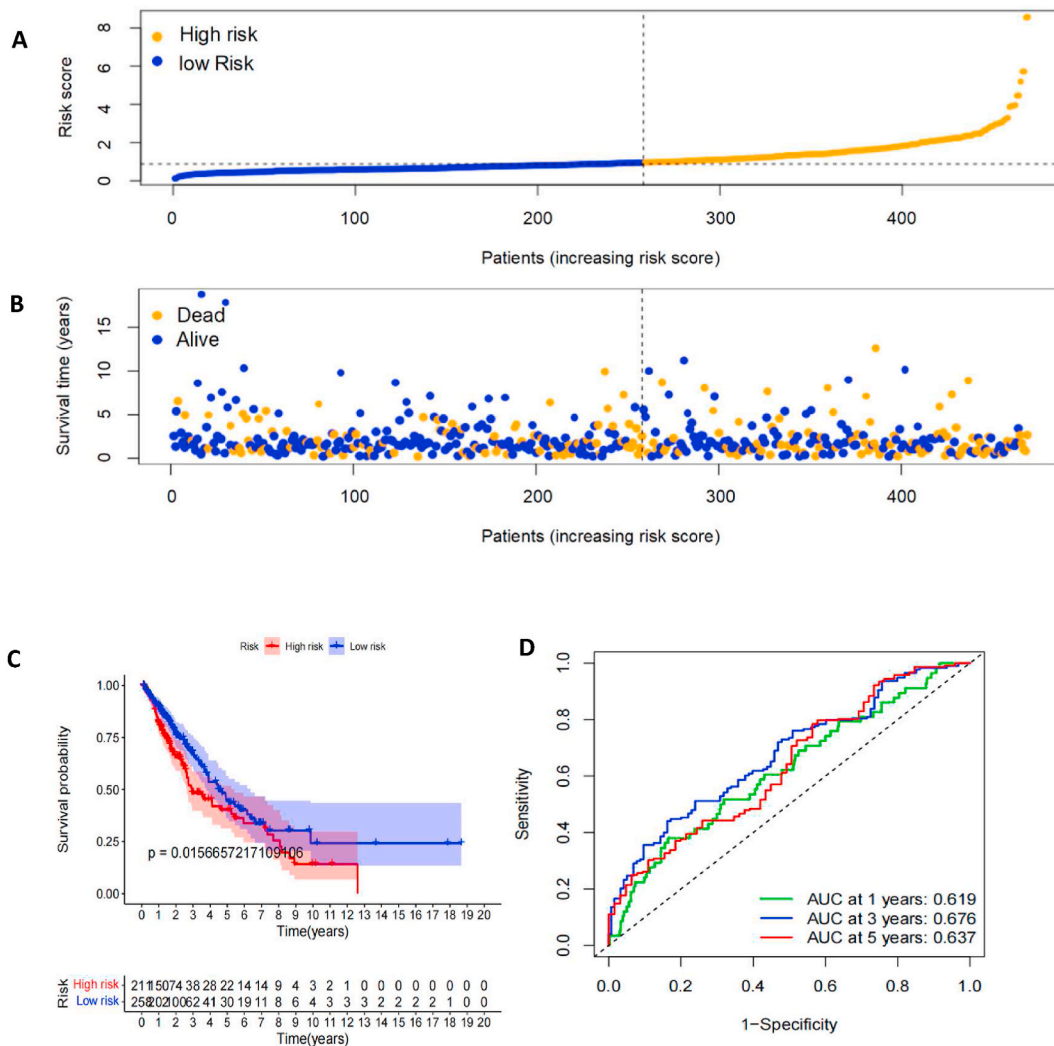


Fig. 4. Evaluation of signature within the validation dataset. (A) Allocation of risk ratings between high and low-risk categories. High-risk and low-risk were indicated by orange and blue points, in that order. **(B)** Allocation of survival rates among NSCLC patients categorized into high/low risk groups. A blue dot signified life and an orange dot denoted death. **(C)** Curve depicting survival. The survival rates of the high and low risk groups were depicted by the red and blue lines, in that order. **(D)** ROC Curve. (For interpretation of the references to colour in this figure legend, the reader is referred to the Web version of this article.)

patient.

3.6. Variations in cellular senescence status among groups with low and high risk

Subsequently, PCA was conducted to evaluate the low versus high-risk categories based on the entire genome, cellular aging-related mRNAs, and the risk model. mRNAs, whether encompassing the entire genome or linked to aging, fail to effectively differentiate between populations at high and low risk (Fig. 7A and B). Nonetheless, employing cellular senescence-related mRNAs distinctly differentiates between patients at high and low risk, thereby reinforcing the model's precision (Fig. 7C). The findings suggest that mRNAs linked to cellular aging independently predict the risk for NSCLC patients.

3.7. GSEA functional analysis

The GSEA technique was employed for additional functional annotation. Altogether, 5569 GO (Table S5) terms and 178 KEGG pathways were gathered (Table S6). GO results indicated GOBP_EXPORT_ACROSS_PLASMA_MEMBRANE: This pathway involves the efflux and excretion of substances by cells through the plasma membrane. In NSCLC, the ability of cells to efflux drugs may affect the effectiveness of treatment and drug resistance, thereby affecting tumor cell survival and proliferation.

Fig. 5. Correlation between differential expression of cellular senescence-associated genes and clinicopathological variables. (A) The heatmap depicted 12 predictive cellular senescence-related mRNAs and clinicopathological factors were distributed among the high and low-risk categories. (B) The Kaplan-Meier survival rates for patients in the high/low-risk category were categorized based on various clinicopathological factors. (C) Cellular senescence-related mRNAs in the cohorts stratified by stage, T stage and fustat.

GOBP_NEGATIVE_REGULATION_OF_TORC1_SIGNALING: This pathway involves the negative regulation of TORC1 signaling. TORC1 plays a crucial role as a cellular signaling route in controlling cell growth, metabolism, and proliferation. In NSCLC, aberrant TORC1 signaling may lead to cell proliferation and tumor development. **GOBP_PEPTIDYL_GlutAMIC_ACID_MODIFICATION:** This pathway involves the modification of glutamic acid residues. Modification of glutamate residues can regulate protein function and stability. In NSCLC, aberrant glutamate modification may lead to abnormal function and expression of tumor-related proteins, thereby affecting cell proliferation and viability. **GOBP_POSITIVE_REGULATION_OF_EXTRINSIC_APOPTOTIC_SIGNALING_PATHWAY:** This pathway involves the positive regulation of exogenous apoptotic signaling pathways. Apoptosis is an important cell death mechanism that is essential for maintaining normal cell life cycle and inhibiting tumor growth. In NSCLC, aberrant apoptotic signaling may lead to tumor cell escape and drug resistance. **GOBP_REGULATION_OF_TORC1_SIGNALING:** This pathway is involved in the regulation of TORC1 signaling. As mentioned earlier, the process of TORC1 signaling plays a role in controlling cellular growth, metabolic activities, and proliferation. In NSCLC, abnormalities in the regulation of TORC1 signaling may lead to abnormalities in cell proliferation and tumor development (Fig. 8A).

KEGG results indicated that **KEGG_ABC_TRANSPORTERS:** The pathway encompasses a group of ABC transporters crucial in controlling the movement and elimination of substances within cells at the membrane. Within NSCLC, the role of ABC transporters could extend to drug transportation and the development of drug resistance, significantly contributing to the chemosensitivity of cancer cells. **KEGG_ADHERENS_JUNCTION:** The pathway plays a role in forming and sustaining adherens junctions among cells. In NSCLC, abnormal intercellular adhesion junctions may lead to abnormal cell separation and enhanced metastatic ability, thereby promoting tumor invasion and metastasis. **KEGG_ALDOSTERONE_REGULATED_SODIUM_REABSORPTION:** the pathways involved in regulation of aldosterone sodium reabsorption process. Although it is more common in non-lung tissues, in NSCLC, some research indicates that aldosterone and its associated mechanisms might contribute to the development and spread of tumors. However, the specific mechanisms of this need to be further investigated. **KEGG_ALPHA_LINOLENIC_ACID_METABOLISM:** This pathway is involved in α -linolenic acid metabolism. As a polyunsaturated fatty acid, linolenic acid has significant anti-inflammatory and antioxidant properties. For NSCLC, irregular lipid metabolism can impact the growth and longevity of cancer cells, encompassing linolenic acid and its metabolic routes. **KEGG_AMINO_SUGAR_AND_NUCLEOTIDE_SUGAR_METABOLISM:** This route plays a role in the metabolism of amino and nucleotide sugars. Amino and nucleotide sugars are important carbon and energy sources in cells, and also participate in the synthesis of glycoproteins and glycans. Abnormal amino sugar and nucleotide sugar metabolism may play a role in cell growth and proliferation in NSCLC (Fig. 8B).

3.8. Correlation of prognostic prediction models and immunoassays

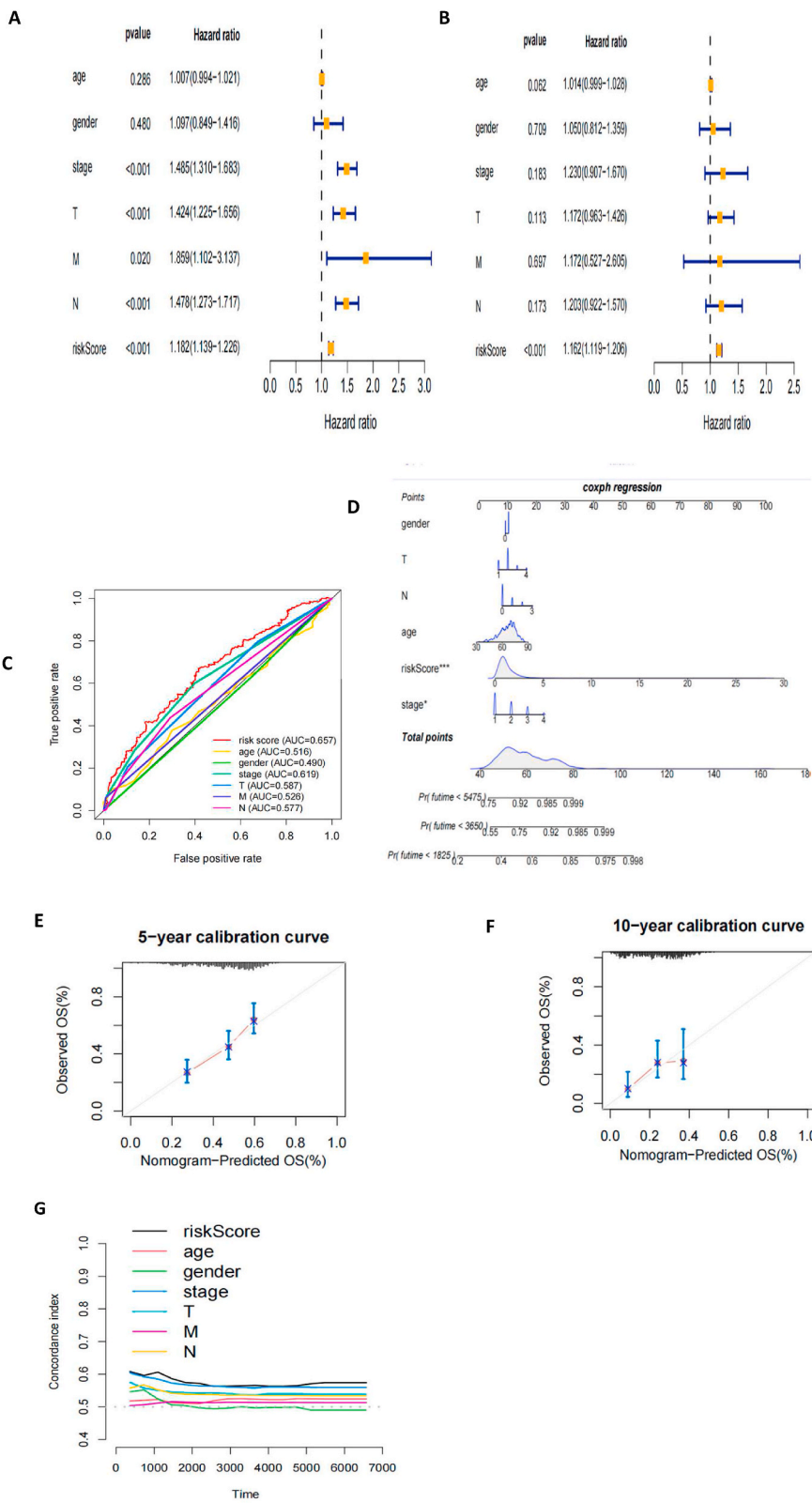
We want to know whether the expression of cellular senescence-associated risk model mRNAs are related to the immune infiltration of NSCLC. Subsequently, the collected samples were split into two segments based on the expression levels of mRNAs within the risk model. Utilizing the CIBERSOFT algorithm and ssGSEA, the gene expression patterns of the acquired samples were examined, leading to the deduction of scores for 22 immune infiltrations. In Fig. 9A, the spread of 22 varieties of immune cells within the sample is depicted (Fig. 9A–Table S7). Immunocyte infiltration was higher in the low-risk group but reduced in the high-risk group. Subsequently, a violin map was developed, revealing variances in B cell naivety, plasma cells, T cell CD4 memory activated and macrophage M0 in groups categorized by high and low risk (Fig. 9B). The low-risk group exhibited significant immunocyte infiltration, indicating a decrease in malignant tumors and treatment efficacy, implying that our marker is indicative of both the prognosis and the degree of immunocyte infiltration.

For a deeper investigation into the link between risk scores and immune cells and their roles, ssGSEA R software was employed to measure the enrichment scores and associated functions across 16 subsets of immune cells. Findings revealed a notable disparity in immune cell types (like aDCs, B_cells, Mast_cells, Th2_cells) between the high-risk and low-risk groups (Fig. 10A). Furthermore, regarding immune performance, there was a notable rise in the scores of HLA, MHC_I, parainflammation, and other immune activities among the high-risk group (Fig. 10B).

To delve deeper into the link between the risk score and 47 immune checkpoint inhibitor (ICI) genes, we conducted an in-depth analysis of the ICI gene expression patterns across these two risk categories (Fig. 11). Findings showed a tendency for low-risk patients to exhibit genes with elevated immune checkpoint functions. The findings suggest that mRNAs linked to cell aging could act as immune checkpoints and/or as indicators of ligand expression and predictive markers for ICIs treatment outcomes.

3.9. Visual examination of TIDE score of immune escape

The TIDE technique was employed to evaluate the prospective clinical effectiveness of immunotherapy across various models. As the TIDE prediction score increases, so does the likelihood of immune evasion, suggesting a reduced probability of patients gaining from ICIs therapy. Findings indicate the high-risk group's TIDE score surpassed that of the low-risk group, implying that ICIs treatment offered lesser advantages to patients in the high-risk category compared to those in the low-risk segment. Consequently, the outlook for



(caption on next page)

Fig. 6. Evaluating risk elements and developing a predictive nomogram. (A) To identify risk factors, both univariate and (B) multivariate analyses were employed. (C) Graphs depicting the AUC and ROC for the risk score alongside clinical variables. Factors in clinical practice include: age, gender, stage, T, N, and M. (D) The prognosis of NSCLC patients is forecasted by a nomogram that considers factors like age, gender, stage, T/N/M stage, and risk score. (E–F) Nomogram's calibration curve. Adjustment graphs used to forecast the total survival rate in NSCLC patients at intervals of 5 years (E) and 10 years (F). As the red solid line approaches the grey solid line, the likelihood of a nomogram's prediction aligns more closely with the real probability. (G) The accuracy of the risk model is assessed by the c-index. (For interpretation of the references to colour in this figure legend, the reader is referred to the Web version of this article.)

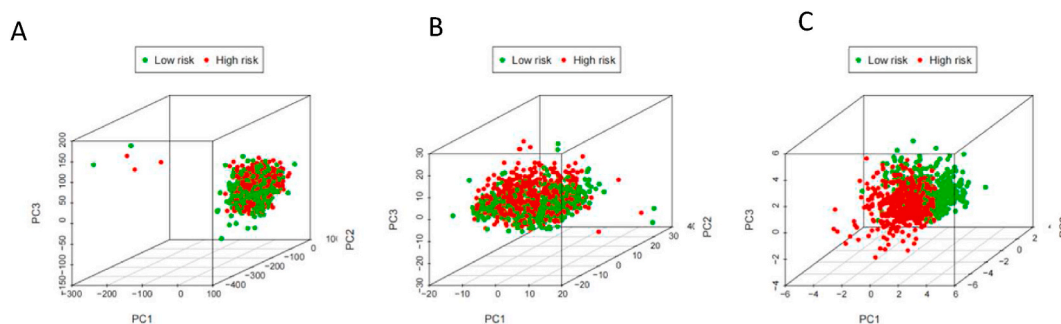


Fig. 7. PCA principal component analysis. (A) Across the genome; (B) The mRNAs associated with cellular senescence; (C) The mRNAs linked to risk models.

the low-risk segment in the model having a reduced TIDE score could be more favorable compared to the high-risk segment (Fig. 12).

4. Discussion

The issue of aging captivates global attention, and the pursuit of anti-aging remains a perpetual endeavor. Concurrently, tumors are an ailment intimately linked to the aging process. The anti-tumor effect of aging and the pro-tumor effect of a certain process are controversial. Based on the age-related accumulation of somatic mutation load and the increase of tumor incidence, Podolskiy et al. proposed that the aging of cells significantly increases the risk of developing tumors [34]. Findings from epidemiological studies indicate that the highest incidence of new cancer cases and fatalities occurs in individuals aged 60 to 74. Within this group, lung cancer ranks as the predominant cancer-related fatality. As one ages, the death rate from lung cancer steadily escalates, anticipated to climax at 80 years old, with the rate continuing to climb. By 2022, cellular aging emerged as a recent indicator of cancer [35–37]. Nonetheless, the process of cellular senescence stands apart from aging, which is possible at any life phase. Aging is indicated by cell senescence, a continual cessation of the cell cycle in response to diverse injury triggers [38]. Certain aging mechanisms might lead to the emergence and progression of cancer, making it crucial to focus on its role as a potent anti-cancer agent. It is anticipated that curbing the unchecked proliferation of impaired cells and impeding cancer progression will emerge as a potent approach in cancer therapy [39,40].

This research primarily aims to examine genes linked to cellular aging in NSCLC, assess how cellular aging correlates with clinicopathological characteristics, prognosis, and treatment outcomes, and to develop a predictive model. This study's examination of genes with varied expressions linked to cell aging encompasses a variety of biological mechanisms and communication routes, mainly involving abnormal gene expression regulation of cell mitosis, cell cycle regulation, cell senescence and other functions and pathways. Consequently, this could play a crucial role in the expansion, multiplication, and spread of lung cancer cells. Therefore, these differentially expressed genes may become potential therapeutic targets or biomarkers. Continued research into the roles and interplays of these signaling routes and genes will enhance comprehension of NSCLC's molecular workings and offer fresh perspectives for diagnosing and treating patients.

Following this, we developed a predictive model for cellular aging-related mRNAs, pinpointed 12 such mRNAs through Lasso and multivariate regression analysis, and computed the risk score. Whether univariate or multivariate analysis, these mRNAs were independently associated with NSCLC prognosis. Subsequently, NSCLC specimens were categorized into groups of low and high risk based on their risk scores, with the penetration of immune cells being a predictor of the effectiveness of immune checkpoint inhibitors. The results suggest that there is a significant degree of immune infiltration in the low-risk group, which partly reflects the reduction and treatment effect of malignant tumors, while the low-risk group tends to express higher immune checkpoint genes. Therefore, the expression characteristics of mRNAs related to cell senescence are not only prognostic markers, but also reflect the ability to predict treatment response and prognosis.

At present, the role and mechanism of cellular senescence in different cancers are still unclear. Althubiti M and colleagues discovered a connection between elevated levels of cell aging markers and the higher survival rates in conditions like glioma, liposarcoma, chronic lymphocytic leukemia, colon cancer, breast cancer and lung cancer through the study of the existing GEO data set [41]. Based on the anti-tumor effect of cell senescence, some scientists have proposed 'combination boxing' therapy, that is, the former drug induces the weakness of tumor cells, and the latter drug attacks this weakness. The physiology of senescent cells is unique in metabolism, secretion, transcriptome and epigenetics. Therefore, the exposed weaknesses are more selective and are therefore

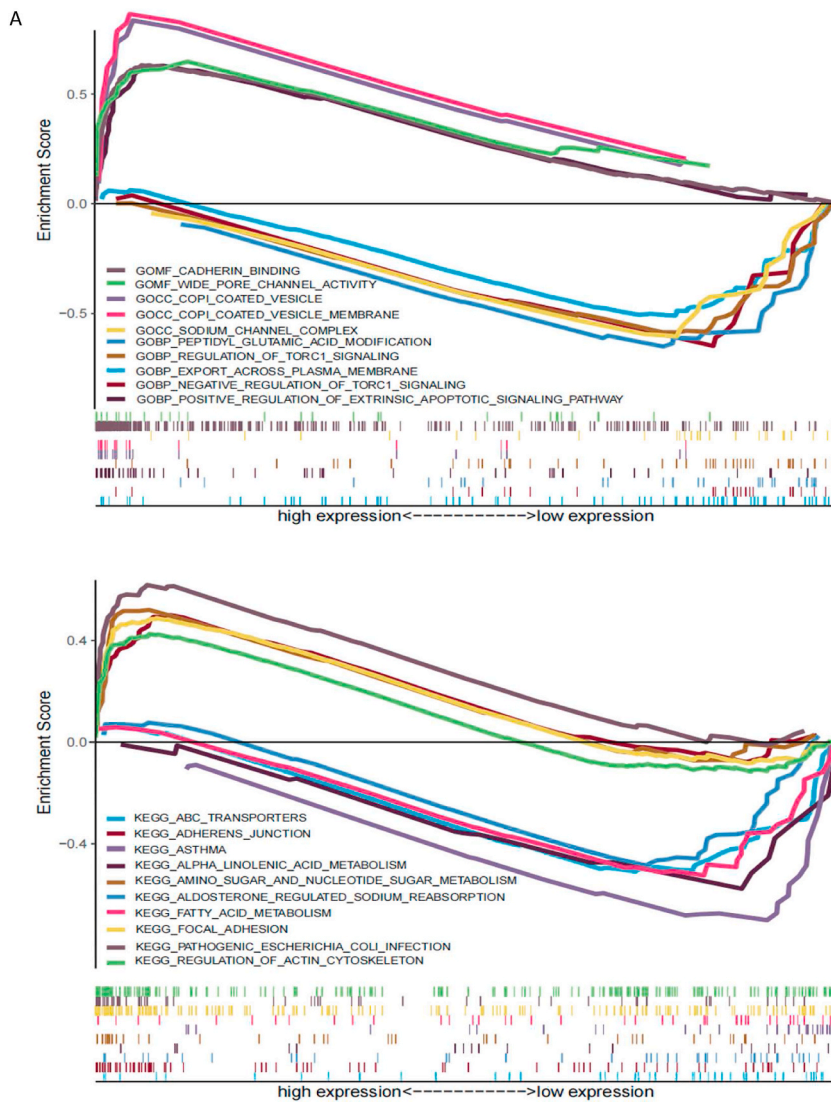


Fig. 8. Gene set enrichment analysis. (A) GO: A notable disparity was observed in the enrichment of 5 GO items between the high and low expression phenotypes, respectively. (B) KEGG: In terms of KEGG items, there was a notable disparity in enrichment between high and low expression phenotypes, as indicated by the normalized enrichment score, nominal p value, and FDR value, respectively.

expected to be part of a sequential treatment regimen [42–44]. Domen A et al. also support such a treatment strategy-assisted anti-aging treatment, anticipated to enhance the survival rates of NSCLC patients exhibiting cellular senescence traits [45]. However, the accumulation of cell senescence in the tumor site, despite cell cycle arrest, senescent cells are in a metabolically active state [44, 46, 47]. However, the accumulation of cellular senescence in the tumor site, although the cell cycle is stagnant, senescent cells are in an active metabolic state, and they exert anti-tumor immunosuppressive effects by continuously secreting a variety of cytokines and chemokines, namely the senescence-associated secretory phenotype SASP [48]. This is a very complex process. Therefore, how to make full use of the positive and negative effects of cell senescence in cancer treatment is worthy of further exploration of its mechanism and functional changes.

Up to this point, precision genomic medicine has concentrated on identifying precise and precise predictors of survival and prognosis using extensive medical data and clinical findings. Utilizing both univariate and multivariate Cox proportional hazard analysis, we determined and calculated the predictive significance of 12 mRNAs risk models linked to cell aging. Additionally, the assessment of the risk scoring approach was conducted using both exploratory and confirmatory techniques. The precision of the predictive model was assessed using the c-index. Findings from this research suggest that a risk model relying on 12 mRNAs associated with cell aging holds more predictive significance compared to other clinicopathological elements. So far, most of the therapeutic drugs for the elderly have been discovered by bioinformatics methods and/or centralized library screening [49]. Therefore, this study has certain clinical transformation value. However, there are no specific markers to detect and quantify aging and senescent cells. In

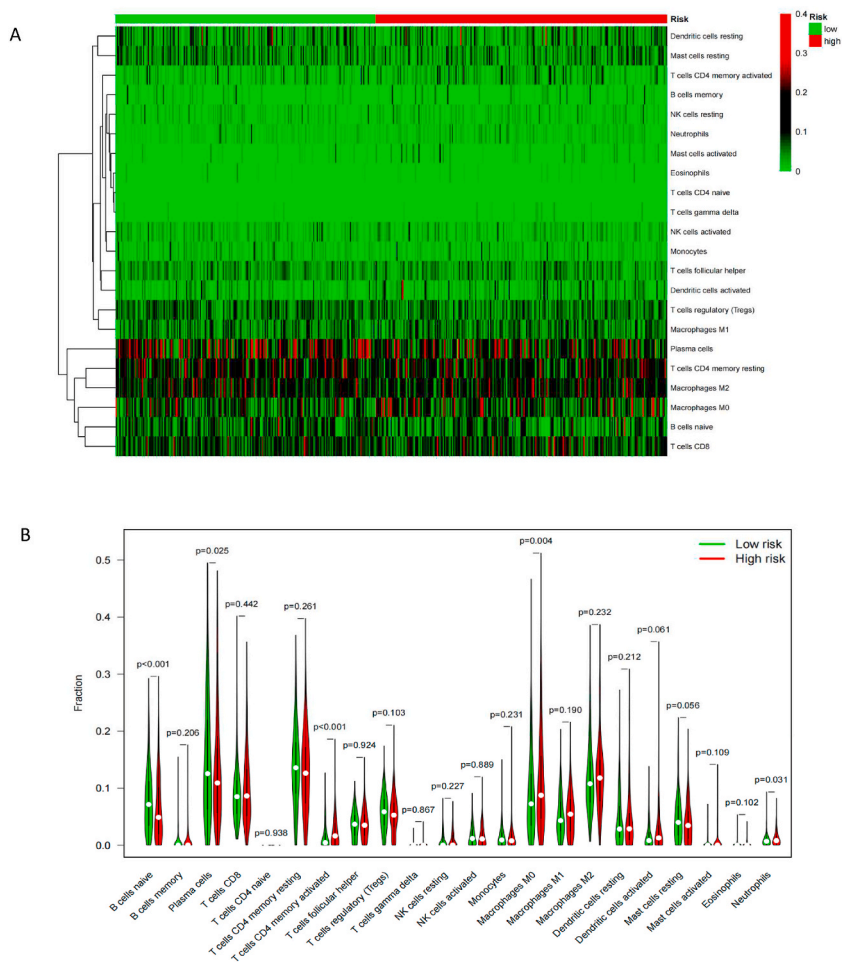


Fig. 9. Immunocyte infiltration analysis. (A) The heatmap displays the penetration of 22 immune cells across various risk samples. **(B)** Variations in the infiltration fractions of 22 immune cells across diverse risk categories.

addition, cellular senescence is highly heterogeneous and complex in terms of cell types, cues, activated signaling pathways, and tissue distribution. Therefore, in the future, we need to consider using some new detection methods, such as AI and neural network models, to further explore the mechanism of cell senescence in diseases (lung cancer), and provide strong support for drug screening and development [50]. In the future, we need to consider the use of some new detection methods, such as AI and neural network models, to further explore the mechanism of cell senescence in diseases, including lung cancer, and provide strong support for drug screening and development.

Present studies are subject to certain constraints. Initially, our focus is on a sole data source (the TCGA database), characterized by its retrospective nature. Additionally, our results were not corroborated by any experimental data conducted in vitro or in vivo. As a third point, standard prognostic indicators like treatment records and tumor biomarkers are excluded from the nomogram due to the incompleteness of the data pertaining to these parameters. Consequently, additional forward-looking research is required to confirm the predictive significance of mRNAs linked to cell aging and to investigate their molecular workings.

5. Conclusion

To conclude, we developed a profile of cellular mRNAs linked to senescence and NSCLC as a predictive tool for prognosis. Concurrently, it's important to acknowledge that the mRNAs linked to cellular aging generated in our research could be connected to the degree of immune penetration and the impact of cancer immunotherapy.

Ethics approval and consent to participate

Not applicable.

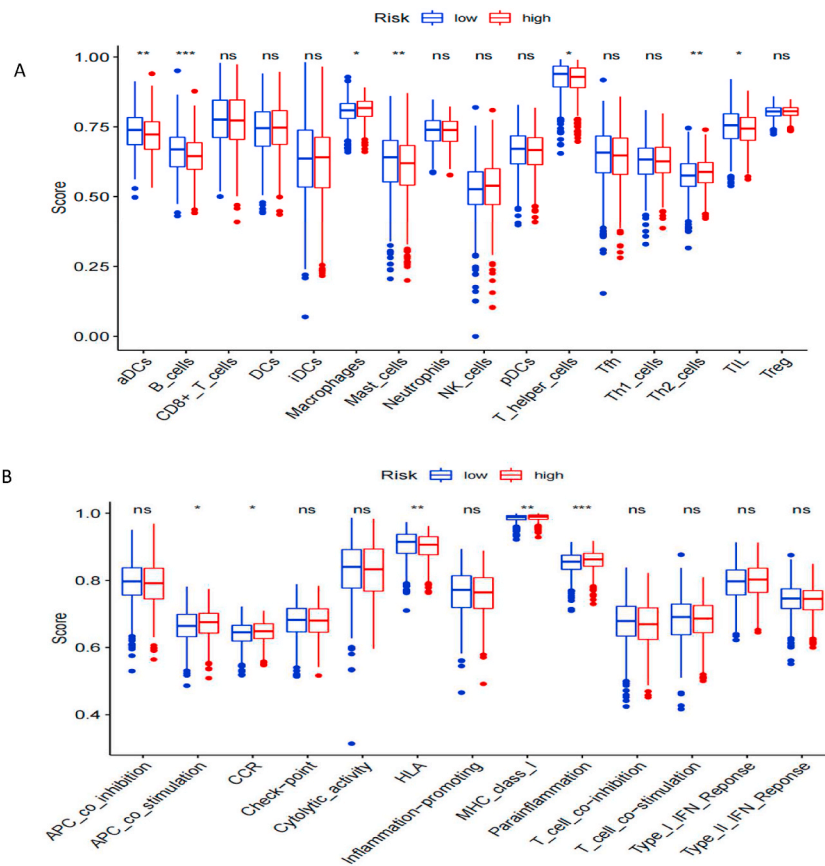


Fig. 10. The relationship between risk scores and the performance of immune cells. (A) Assessment of immune cells across various risk groups. **(B)** The role of immune cells. Red symbolizes a high risk level, while blue indicates a low risk. (*: $p < 0.05$, **: $p < 0.01$, ***: $p < 0.001$). (For interpretation of the references to colour in this figure legend, the reader is referred to the Web version of this article.)

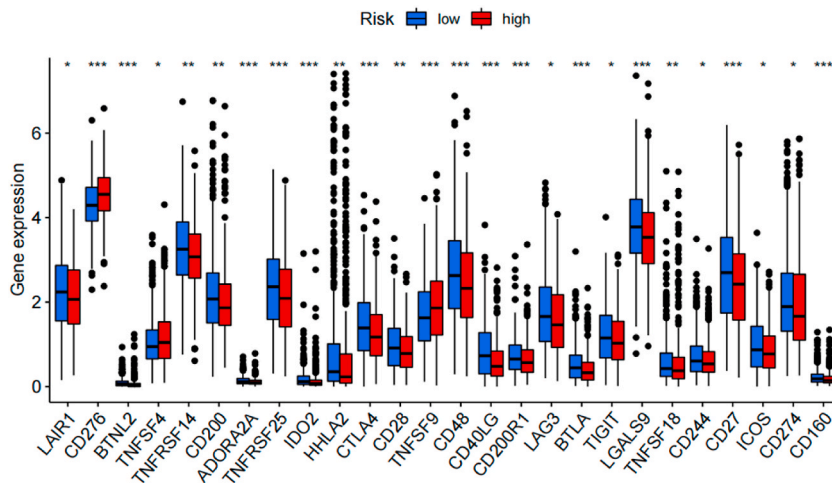


Fig. 11. Correlation of immune checkpoints with mRNA risk models associated with cellular senescence. (*: $p < 0.05$, **: $p < 0.01$, *: $p < 0.001$).**

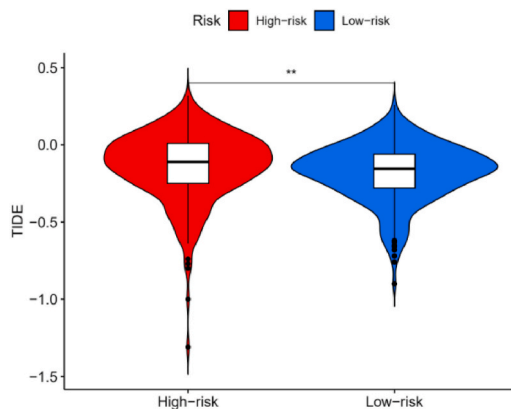


Fig. 12. Scores on the TIDE comparing groups with high and low risks.

Consent for publication

Not applicable.

Declarations of ethics

There's no need for the Ethics Committee to review or approve this research, given that the data is sourced from public databases and the Ethics Committee doesn't need to approve it.

This research did not necessitate informed consent as the participants were sourced from a public database and no additional patients were registered.

Funding

No funding.

Availability of data and materials

The information underpinning the findings can be accessed at the TCGA database (<https://portal.gdc.cancer.gov/>). Genes linked to cellular senescence were sourced from the CellAge database (<https://genomics.Sene-science.info/cells/>).

CRedit authorship contribution statement

Dandan Xu: Writing – original draft, Formal analysis, Data curation, Conceptualization. **Xiao Chen:** Data curation. **Mingyuan Wu:** Investigation. **Jinfeng Bi:** Visualization, Validation, Formal analysis. **Hua Xue:** Supervision. **Hong Chen:** Writing – review & editing, Resources, Methodology.

Declaration of competing interest

The authors declare that they have no known competing financial interests or personal relationships that could have appeared to influence the work reported in this paper.

Acknowledgements

We acquired this study's data from The Cancer Genome Atlas (TCGA) and express our gratitude towards the patients and the surgical procedure. Here, I would like to thank a friend, Wang Li (Professor, Department of Bioinformatics, Harbin Medical University), who taught me about C-index in the process of revising my manuscript.

Appendix A. Supplementary data

Supplementary data to this article can be found online at <https://doi.org/10.1016/j.heliyon.2024.e28278>.

References

- [1] H. Sung, J. Ferlay, R.L. Siegel, et al., Global cancer statistics 2020: GLOBOCAN estimates of incidence and mortality worldwide for 36 cancers in 185 countries, *CA Cancer J Clin* 71 (3) (2021 May) 209–249.
- [2] Rongshou Zheng, Siwei Zhang, Shaoming Wang, et al., Lung cancer incidence and mortality in China: updated statistics and an overview of temporal trends from 2000 to 2016, *Journal of the National Cancer Center* 2 (3) (2022).
- [3] W. Chen, R. Zheng, P.D. Baade, et al., Cancer statistics in China, 2015, *CA Cancer J Clin* 66 (2) (2016 Mar-Apr) 115–132.
- [4] R. Feng, Q. Su, X. Huang, T. Basnet, et al., Cancer situation in China: what does the China cancer map indicate from the first national death survey to the latest cancer registration? *Cancer Commun.* 43 (1) (2023 Jan) 75–86.
- [5] SEER*Explorer, An interactive website for SEER cancer statistics [Internet] [updated: 2023 Jun 8; cited 2023 Sep 7]. Available from::SEER*Explorer Application (cancer.gov), in: Surveillance Research Program, National Cancer Institute, 2023 Apr 19.
- [6] X. Qian, H.Y. Zhang, Q.L. Li, G.J. Ma, Z. Chen, X.M. Ji, C.Y. Li, A.Q. Zhang, Integrated microbiome, metabolome, and proteome analysis identifies a novel interplay among commensal bacteria, metabolites and candidate targets in non-small cell lung cancer, *Clin. Transl. Med.* 12 (6) (2022 Jun) e947.
- [7] A. Rizzo, Identifying optimal first-line treatment for advanced non-small cell lung carcinoma with high PD-L1 expression: a matter of debate, *Br. J. Cancer* 127 (8) (2022 Nov) 1381–1382.
- [8] P. Oster, L. Vaillant, E. Riva, B. McMillan, C. Begka, C. Truntzer, C. Richard, M.M. Leblond, M. Messaoudene, E. Machremi, E. Limagne, F. Ghiringhelli, B. Routy, G. Verdeil, D. Velin, *Helicobacter pylori* infection has a detrimental impact on the efficacy of cancer immunotherapies, *Gut* 71 (3) (2022 Mar) 457–466.
- [9] L. Derosa, M.D. Hellmann, M. Spaziano, D. Halpenny, M. Fidelle, H. Rizvi, N. Long, A.J. Plodkowski, K.C. Arbour, J.E. Chaff, J.A. Rouche, L. Zitvogel, G. Zalman, L. Albiges, B. Escudier, B. Routy, Negative association of antibiotics on clinical activity of immune checkpoint inhibitors in patients with advanced renal cell and non-small-cell lung cancer, *Ann. Oncol.* 29 (6) (2018 Jun 1) 1437–1444.
- [10] A. Elkrief, L. Derosa, G. Kroemer, L. Zitvogel, B. Routy, The negative impact of antibiotics on outcomes in cancer patients treated with immunotherapy: a new independent prognostic factor? *Ann. Oncol.* 30 (10) (2019 Oct 1) 1572–1579.
- [11] L. Lurienne, J. Cervesi, L. Duhalde, J. de Gunzburg, A. Andreumont, G. Zalman, R. Buffet, P.A. Bandinelli, NSCLC immunotherapy efficacy and antibiotic use: a systematic review and meta-analysis, *J. Thorac. Oncol.* 15 (7) (2020 Jul) 1147–1159.
- [12] A. Rizzo, A. Cusmai, F. Giovannelli, S. Acquafredda, L. Rinaldi, A. Misino, E.S. Montagna, V. Ungaro, M. Lorusso, G. Palmiotti, Impact of proton pump inhibitors and Histamine-2-Receptor antagonists on non-small cell lung cancer immunotherapy: a systematic review and meta-analysis, *Cancers* 14 (6) (2022 Mar 9) 1404.
- [13] L. Eng, R. Sutradhar, Y. Niu, N. Liu, Y. Liu, Y. Kaliwal, M.L. Powis, G. Liu, J.M. Peppercorn, P.L. Bedard, M.K. Krzyzanowska, Impact of antibiotic exposure before immune checkpoint inhibitor treatment on overall survival in older adults with cancer: a population-based study, *J. Clin. Oncol.* 41 (17) (2023 Jun 10) 3122–3134.
- [14] M. Santoni, A. Rizzo, V. Mollica, M.R. Matrana, M. Rosellini, L. Faloppi, A. Marchetti, N. Battelli, F. Massari, The impact of gender on the efficacy of immune checkpoint inhibitors in cancer patients: the MOUSEION-01 study, *Crit. Rev. Oncol. Hematol.* 170 (2022 Feb) 103596.
- [15] M. Szczyrek, P. Bitkowska, P. Chunowski, P. Czuchryta, P. Krawczyk, J. Milanowski, Diet, microbiome, and cancer immunotherapy-A comprehensive review, *Nutrients* 13 (7) (2021 Jun 28) 2217.
- [16] R.S. Herbst, D. Morgensztern, C. Boshoff, The biology and management of non-small cell lung cancer, *Nature* 553 (7689) (2018 Jan 24) 446–454.
- [17] L. Hayflick, P.S. Moorhead, The serial cultivation of human diploid cell strains, *Exp. Cell Res.* 25 (1961 Dec) 585–621.
- [18] J. Campisi, F. d'Adda di Fagagna, Cellular senescence: when bad things happen to good cells, *Nat. Rev. Mol. Cell Biol.* 8 (9) (2007 Sep) 729–740.
- [19] F. d'Adda di Fagagna, Living on a break: cellular senescence as a DNA-damage response, *Nat. Rev. Cancer* 8 (7) (2008 Jul) 512–522.
- [20] C.D. Wiley, M.C. Velarde, P. Lecot, et al., Mitochondrial dysfunction induces senescence with a distinct secretory phenotype, *Cell Metabol.* 23 (2) (2016 Feb 9) 303–314.
- [21] S. Miwa, S. Kashyap, E. Chini, et al., Mitochondrial dysfunction in cell senescence and aging, *J. Clin. Invest.* 132 (13) (2022 Jul 1) e158447.
- [22] M. Serrano, A.W. Lin, M.E. McCurrach, et al., Oncogenic ras provokes premature cell senescence associated with accumulation of p53 and p16INK4a, *Cell* 88 (5) (1997 Mar 7) 593–602.
- [23] C. Chandeeck, W.J. Mooi, Oncogene-induced cellular senescence, *Adv. Anat. Pathol.* 17 (1) (2010 Jan) 42–48.
- [24] V. Gorgoulis, P.D. Adams, A. Alimonti, et al., Cellular senescence: defining a path forward, *Cell* 179 (4) (2019 Oct 31) 813–827.
- [25] D. Hanahan, R.A. Weinberg, The hallmarks of cancer, *Cell* 100 (1) (2000 Jan 7) 57–70.
- [26] D. Hanahan, R.A. Weinberg, Hallmarks of cancer: the next generation, *Cell* 144 (5) (2011 Mar 4) 646–674.
- [27] F. Rodier, J. Campisi, Four faces of cellular senescence, *J. Cell Biol.* 192 (4) (2011 Feb 21) 547–556.
- [28] M.J. Regulski, Cellular senescence: what, why, and how, *Wounds* 29 (6) (2017 Jun) 168–174.
- [29] J. Campisi, Aging, cellular senescence, and cancer, *Annu. Rev. Physiol.* 75 (2013) 685–705.
- [30] J.L. Schneider, J.H. Rowe, C. Garcia-de-Alba, C.F. Kim, A.H. Sharpe, M.C. Haigis, The aging lung: physiology, disease, and immunity, *Cell* 184 (8) (2021 Apr 15) 1990–2019.
- [31] X. Zhao, X. Liu, L. Cui, Development of a five-protein signature for predicting the prognosis of head and neck squamous cell carcinoma, *Aging (Albany NY)* 12 (19) (2020 Oct 13) 19740–19755.
- [32] Q. Yao, X. Zhang, C. Wei, H. Chen, Q. Xu, J. Chen, D. Chen, Prognostic prediction and immunotherapy response analysis of the fatty acid metabolism-related genes in clear cell renal cell carcinoma, *Heliyon* 9 (6) (2023 Jun 13) e17224.
- [33] Y. Guo, Z. Qu, D. Li, F. Bai, J. Xing, Q. Ding, J. Zhou, L. Yao, Q. Xu, Identification of a prognostic ferroptosis-related lncRNA signature in the tumor microenvironment of lung adenocarcinoma, *Cell Death Dis.* 7 (1) (2021 Jul 26) 190.
- [34] D.I. Podolskiy, A.V. Lobanov, G.V. Kryukov, et al., Analysis of cancer genomes reveals basic features of human aging and its role in cancer development, *Nat. Commun.* 7 (2016 Aug 12) 12157.
- [35] K. Poropatich, J. Fontanarosa, S. Samant, et al., Cancer immunotherapies: are they as effective in the elderly? *Drugs Aging* 34 (8) (2017 Aug) 567–581.
- [36] D. Hashim, G. Carioli, M. Malvezzi, et al., Cancer mortality in the oldest old: a global overview, *Aging (Albany NY)* 12 (17) (2020 Sep 3) 16744–16758.
- [37] M.V. Blagosklonny, Hallmarks of cancer and hallmarks of aging, *Aging (Albany NY)* 14 (9) (2022 May 9) 4176–4187, <https://doi.org/10.18632/aging.204082>. Epub 2022 May 9.
- [38] A. Calcinotto, J. Kohli, E. Zagato, et al., Cellular senescence: aging, cancer, and injury, *Physiol. Rev.* 99 (2) (2019 Apr 1) 1047–1078.
- [39] J.P. de Magalhães, How ageing processes influence cancer, *Nat. Rev. Cancer* 13 (5) (2013 May) 357–365.
- [40] J.M. van Deursen, The role of senescent cells in ageing, *Nature* 509 (7501) (2014 May 22) 439–446.
- [41] M. Althubiti, L. Lezina, S. Carrera, et al., Characterization of novel markers of senescence and their prognostic potential in cancer, *Cell Death Dis.* 5 (11) (2014 Nov 20) e1528.
- [42] J.C. Acosta, J. Gil, Senescence: a new weapon for cancer therapy, *Trends Cell Biol.* 22 (4) (2012 Apr) 211–219.
- [43] L. Wang, R. Bernards, Taking advantage of drug resistance, a new approach in the war on cancer, *Front. Med.* 12 (4) (2018 Aug) 490–495.
- [44] L. Wang, L. Lankhorst, R. Bernards, Exploiting senescence for the treatment of cancer, *Nat. Rev. Cancer* (2022) 340–355.
- [45] A. Domen, C. Deben, I. De Pauw, et al., Prognostic implications of cellular senescence in resected non-small cell lung cancer, *Transl. Lung Cancer Res.* 11 (8) (2022 Aug) 1526–1539.
- [46] J.R. Dörr, Y. Yu, M. Milanovic, et al., Synthetic lethal metabolic targeting of cellular senescence in cancer therapy, *Nature* 501 (7467) (2013 Sep 19) 421–425.
- [47] L. Roger, F. Tomas, V. Gire, Mechanisms and regulation of cellular senescence, *Int. J. Mol. Sci.* 22 (23) (2021 Dec 6) 13173.

- [48] T. Eggert, K. Wolter, J. Ji, et al., Distinct functions of senescence-associated immune responses in liver tumor surveillance and tumor progression, *Cancer Cell* 30 (4) (2016 Oct 10) 533–547.
- [49] L. Zhang, L.E. Pitcher, V. Prahalad, L.J. Niedernhofer, P.D. Robbins, Targeting cellular senescence with senotherapeutics: senolytics and senomorphics, *FEBS J.* 290 (5) (2023 Mar) 1362–1383.
- [50] L. Zhang, L.E. Pitcher, M.J. Yousefzadeh, L.J. Niedernhofer, P.D. Robbins, Y. Zhu, Cellular senescence: a key therapeutic target in aging and diseases, *J. Clin. Invest.* 132 (15) (2022 Aug 1) e158450.